HHS Public Access

Author manuscript

Science. Author manuscript; available in PMC 2017 April 06.

Published in final edited form as:

Science. 2017 January 06; 355(6320): 84–88. doi:10.1126/science.aah4307.

SOX2 promotes lineage plasticity and antiandrogen resistance in *TP53*- and *RB1*-deficient prostate cancer

Ping Mu[1], **Zeda Zhang**[1,2], **Matteo Benelli**[3], **Wouter R. Karthaus**[1], **Elizabeth Hoover**[1], **Chi-Chao Chen**[4,5], **John Wongvipat**[1], **Sheng-Yu Ku**[6], **Dong Gao**[1], **Zhen Cao**[1,5], **Neel Shah**[1,2], **Elizabeth J. Adams**[1], **Wassim Abida**[1], **Philip A. Watson**[1], **Davide Prandi**[3], **Chun-Hao Huang**[4,5], **Elisa de Stanchina**[7], **Scott W. Lowe**[4,5,8], **Leigh Ellis**[6], **Himisha Beltran**[9,10], **Mark A. Rubin**[9,10], **David W. Goodrich**[6], **Francesca Demichelis**[3,9], and **Charles L. Sawyers**[1,8,*]

[1]Human Oncology and Pathology Program, Memorial Sloan Kettering Cancer Center, 1275 York Avenue, New York, NY 10065, USA

[2]Louis V. Gerstner, Jr. Graduate School of Biomedical Sciences, Memorial Sloan Kettering Cancer Center, New York, NY 10065, USA

[3]Centre for Integrative Biology, University of Trento, Trento, Italy

[4]Cancer Biology and Genetics Program, Memorial Sloan Kettering Cancer Center, 1275 York Avenue, New York, NY 10065, USA

[5]Weill Cornell Graduate School of Medical Sciences of Cornell University, New York, NY 10021, USA

[6]Department of Pharmacology and Therapeutics, Roswell Park Cancer Institute, New York, NY 14263, USA

[7]Department of Molecular Pharmacology, Memorial Sloan Kettering Cancer Center, 1275 York Avenue, New York, NY 10065, USA

[8]Howard Hughes Medical Institute, Chevy Chase, MD 20815, USA

[9]Englander Institute for Precision Medicine, Weill Cornell Medicine and New York Presbyterian Hospital, New York, NY 10065, USA

[10]Sandra and Edward Meyer Cancer Center at Weill Cornell Medicine, New York, NY 10021, USA

Abstract

Some cancers evade targeted therapies through a mechanism known as lineage plasticity, whereby tumor cells acquire phenotypic characteristics of a cell lineage whose survival no longer depends on the drug target. We use in vitro and in vivo human prostate cancer models to show that these

*Corresponding author. sawyersc@mskcc.org.

SUPPLEMENTARY MATERIALS

www.sciencemag.org/content/355/6320/84/suppl/DC1

Materials and Methods

Figs. S1 to S11

Tables S1 to S3

References (*31*–*39*)

tumors can develop resistance to the antiandrogen drug enzalutamide by a phenotypic shift from androgen receptor (AR)–dependent luminal epithelial cells to AR-independent basal-like cells. This lineage plasticity is enabled by the loss of TP53 and RB1 function, is mediated by increased expression of the reprogramming transcription factor *SOX2*, and can be reversed by restoring TP53 and RB1 function or by inhibiting *SOX2* expression. Thus, mutations in tumor suppressor genes can create a state of increased cellular plasticity that, when challenged with antiandrogen therapy, promotes resistance through lineage switching.

Evading cancer drugs by identity fraud

Prostate cancer growth is fueled by male hormones called androgens. Drugs targeting the androgen receptor (AR) are initially efficacious, but most tumors eventually become resistant (see the Perspective by Kelly and Balk). Mu *et al*. found that prostate cancer cells escaped the effects of androgen deprivation therapy through a change in lineage identity. Functional loss of the tumor suppressors TP53 and RB1 promoted a shift from AR-dependent luminal epithelial cells to AR-independent basal-like cells. In related work, Ku *et al*. found that prostate cancer metastasis, lineage switching, and drug resistance were driven by the combined loss of the same tumor suppressors and were accompanied by increased expression of the epigenetic regulator Ezh2. Ezh2 inhibitors reversed the lineage switch and restored sensitivity to androgen deprivation therapy in experimental models.

Resistance to targeted cancer therapies is often caused by mutations in the drug target, typified by gatekeeper mutations in *epidermal growth factor receptor* (*EGFR*)–mutant lung cancer, *BCR-ABL* positive leukemias, and several other cancers treated with kinase inhibitors (1, 2). An alternative escape mechanism is to restore signaling downstream of the pharmacologic blockade through activation of a bypass pathway, as observed in *BRAF*-mutant melanoma (3). Elucidation of the molecular details underlying these mechanisms has stimulated the development of next-generation inhibitors, as well as combinations of inhibitors to prevent or delay resistance.

There is now increasing recognition of a third mechanism, whereby tumor cells acquire resistance by switching lineages from a cell type that is dependent on the drug target to a different cell type that is not. One example is relapse of *EGFR*-mutant lung adenocarcinoma as small cell carcinoma after treatment with EGFR inhibitors (4). This ability to undergo a phenotypic switch from an epithelial cell to a neuroendocrine cell is often called lineage plasticity. In addition to tumors treated with kinase inhibitors, there is evidence of lineage plasticity in metastatic prostate cancers treated with antiandrogen therapy. Like lung cancer, some patients with castration-resistant prostate cancer (CRPC) relapse with tumor cells that have some morphologic features of neuroendocrine carcinoma but mixed luminal and basal epithelial characteristics (5). The mechanism by which lineage plasticity confers cancer drug resistance is poorly understood.

A recent genomic landscape analysis of prostate cancer revealed that alterations in two genes, androgen receptor (*AR*) and *TP53*, are greatly enriched in metastatic CRPC relative to primary prostate cancer (6). The increased frequency of *AR* alterations was expected on the basis of long-standing evidence that elevated *AR* expression confers resistance to

castration therapy (7), but the presence of *TP53* alterations in half of all CRPC cases was not anticipated, other than in an older small-case series (8). To determine whether the loss of TP53 function confers antiandrogen resistance, we introduced stable short hairpin RNAs (shRNAs) targeting *TP53* into LNCaP/AR prostate cancer cells, a wild-type (WT) *TP53* model that is highly sensitive to the next-generation antiandrogen enzalutamide (9). This model has previously revealed resistance mechanisms, such as AR mutation or glucocorticoid overexpression, that are now observed in patients (10, 11). Although *TP53* knockdown caused a modest reduction in enzalutamide sensitivity of LNCaP/AR cells grown in vitro, no effect was observed in another WT *TP53* human prostate cancer model (CWR22Pc-EP) or in LNCaP/AR xenografts (Fig. 1, A to C, and fig. S1). Therefore, we conclude that *TP53* loss of function alone is not sufficient to confer enzalutamide resistance.

We next considered the possibility that a second genomic alteration, in addition to the *TP53* mutation, might be required. Examination of three primary and metastatic CRPC genomic data sets [The Cancer Genome Atlas, Stand Up To Cancer (SU2C), Institute for Precision Medicine (IPM)–Cornell] for co-occurring events (6, 12, 13) revealed *RB1* and *PTEN* as potential candidates. *RB1* was of particular interest because combined loss of *TP53* and *RB1* has been well documented in neuroendocrine cancers of various tissue origins, including neuroendocrine-like prostate cancer (14, 15). Furthermore, conditional *Tp53* and *Rb1* deletion in mice is sufficient to generate cancers from various tissue origins, including prostate, often with neuroendocrine histology (16, 17). Meta-analysis of these data sets revealed that concurrent *TP53* and *RB1* alterations were present in 5% of primary cancers, 39% of metastatic CRPCs with adenocarcinoma histology, and 74% of metastatic CRPCs with neuroendocrine-like histology (Fig. 1D). Treatment data were available from a subset of cases in the IPM-Cornell cohort and revealed that the frequency of combined *TP53* and *RB1* alteration was significantly higher in tumors from men whose disease had progressed on treatment with enzalutamide or the androgen synthesis inhibitor abiraterone (Fig. 1E), consistent with the hypothesis that *TP53* and *RB1* loss of function confers resistance.

We therefore returned to the LNCaP/AR and CWR22Pc-EP models to examine the consequences of single versus combined *TP53* and *RB1* knockdown on enzalutamide resistance. In contrast to the modest effects of single knockdown, combined knockdown conferred nearcomplete enzalutamide resistance in both models, as measured by proliferation and EdU incorporation in vitro and tumor xenograft growth in vivo (Fig. 1, A to C, and figs. S1 and S2). Similar results were observed in culture and xenograft assays by deletion of *TP53* and *RB1* using CRISPR-Cas9 in LNCaP/AR cells (fig. S3), as well as in primary mouse prostate organoids derived from $Trp53^{loxP/loxP}$, $Rb1^{loxP/loxP}$ mice after infection with Cre-expressing lentivirus (fig. S4). One surprising feature of enzalutamide resistance caused by *TP53* and *RB1* loss was sustained inhibition of AR target genes such as *NKX3.1, TMPRSS2, FKBP5, NDRG1* and *TIPARP*, despite vigorous growth of tumor xenografts (Fig. 1F). This observation contrasts with the more common resistance phenotype of restored AR pathway signaling—as seen with *AR* mutation, *AR* amplification, or glucocorticoid receptor (GR) bypass—and suggests an AR-independent resistance mechanism, despite robust AR expression.

To further evaluate this resistance phenotype, we surveyed the expression of canonical genes that define the luminal, basal, and neuroendocrine cell types present in normal prostate tissue. LNCaP/AR and CWR22Pc-EP cells with combined shRNA knockdown of *TP53* and *RB1*, but not single *TP53* or *RB1* knockdown, had a 5- to 10-fold increase in expression of basal (*CK5, CK14*, and *TP63*) and neuroendocrine markers (*SYP* and *CHGA*) and reduced expression of luminal cell markers (*AR, CK8*, and *CK18*). These expression changes were also evident at the protein level in cultured cells (Western blot and immunofluorescence), in xenografts (RNA and immunohistochemistry), and in LNCaP/AR cells after CRISPR-Cas9–mediated *TP53* and *RB1* deletion (Fig. 2, A and B, and fig. S5). In addition, global transcriptome profiling by RNA sequencing (RNA-seq) revealed significant enrichment of basal-signature genes after knockdown of *TP53* and *RB1* (Fig. 2C). Because luminal prostate epithelial cells are dependent on AR for survival and basal epithelial cells are not, we hypothesize that the loss of *TP53* and *RB1* function confers antiandrogen resistance by promoting a state of lineage plasticity that, in response to drug treatment, enables expansion of tumor cells with basal epithelial features that no longer require AR function to proliferate.

To determine the kinetics of this lineage plasticity phenotype, we turned to a doxycycline-inducible shRNA knockdown model. Increased expression of basal and neuroendocrine lineage markers was evident within 48 hours of doxycycline addition, with concurrent acquisition of enzalutamide resistance when scored 7 days later (Fig. 2, D to F). Furthermore, these changes in lineage gene expression shifted back to a more luminal state when *TP53* and *RB1* amounts reached baseline levels after doxycycline withdrawal (fig. S6A). Consistent with the effect on antiandrogen resistance, the most dramatic changes in lineage marker expression occurred after knockdown of both genes (fig. S6B). The rapidity and reversibility of these changes suggest a population-wide shift in lineage plasticity rather than emergence of a rare subpopulation of enzalutamide-resistant cells under selective pressure.

Transcription factors (TFs) function as master regulators of lineage development in multiple tissues. To determine whether lineage plasticity in prostate cancer might also be explained by aberrant TF expression, we examined RNA-seq data from the IPM-Cornell (12) and SU2C (6) metastatic CRPC cohorts for differential expression of TFs in $TP53^{WT}$, $RB1^{WT}$ versus $TP53^{Alt}$, $RB1^{Alt}$ tumors. We found that mRNA levels of eight TFs were significantly higher in $TP53^{Alt}$, $RB1^{Alt}$ tumors across the two data sets (Fig. 3A). Of these, *SOX2* showed the greatest and most consistent change (3.6-fold increase) and had the lowest baseline expression in $TP53^{WT}$, $RB1^{WT}$ tumors relative to the other seven genes (Fig. 3B). Examination of *SOX2* in individual tumors revealed low to absent expression in $TP53^{WT}$, $RB1^{WT}$ tumors, with up to 25-fold higher levels in $TP53^{Alt}$, $RB1^{Alt}$ cancers (Fig. 3C). *SOX2* levels were also significantly higher in CRPC tumors with neuroendocrine-like histology versus adenocarcinoma (fig. S7), consistent with the higher frequency of *TP53* and *RB1* alteration in this subtype (74 versus 39%; Fig. 1D).

Having documented this association between *TP53* and *RB1* alteration and *SOX2* expression in human prostate tumors, we next asked whether impairment of *TP53* and *RB1* function in $TP53^{WT}$, $RB1^{WT}$ prostate cells is sufficient to induce *SOX2* expression. We observed 10- to 50-fold up-regulation of *SOX2* in the LNCaP/AR and CWR22Pc-EP models after *TP53* and

RB1 knockdown or CRISPR deletion and in primary *Trp53*$^{loxP/loxP}$, *Rb1*$^{loxP/loxP}$ mouse prostate after *Trp53* and *Rb1* deletion (Fig. 3, D to F, and fig. S8, A and B). *SOX2* up-regulation was rapid (48 hours) and required the loss of function of both *TP53* and *RB1* (Fig. 3G and fig. S8, C and D). Of the eight TFs differentially expressed in *TP53*^{Alt}, *RB1*^{Alt} tumors (Fig. 3A), only *SOX2* was up-regulated in these model systems (fig. S9). It has been suggested that AR directly represses *SOX2* in prostate cells, raising the possibility that antiandrogen therapy might directly promote lineage plasticity (18). We found that enzalutamide did not induce *SOX2* in parental LNCaP/AR cells, whereas combined *TP53* and *RB1* knockdown resulted in >15-fold up-regulation. Of note, treatment with enzalutamide after knockdown of *TP53* and *RB1* caused a modest (0.4-fold) additional increase in *SOX2* levels (fig. S10A). Chromatin immunoprecipitation analysis showed strong, enzalutamide-reversible AR binding at canonical AR target gene loci such as *KLK3* and *FKBP5*, but not at *SOX2* (fig. S10B). We conclude that TP53 and RB1 are the primary regulators of SOX2 in this model and that lineage plasticity observed in the context of combined TP53 and RB1 is not caused by AR inhibition.

SOX2 is one of four TFs involved in reprogramming fibroblasts to induced pluripotent stem (iPS) cells (19) and has been implicated as a driver in squamous epithelial cancers through gene amplification (20, 21) and as a marker of neuroendocrine differentiation in prostate cancer (21, 22). Because the lineage plasticity associated with the observable loss of *TP53* and *RB1* in our model systems shares features with reprogramming, we asked whether *SOX2* is required for this phenotype. shRNA knockdown of *SOX2* in LNCaP/AR tumor cells with inactivation of *TP53* and *RB1* completely reversed the increased expression of basal (*CK5, CK14*, and *TP63*) and neuroendocrine (*SYP, CHGA*, and *NSE*) lineage markers induced by the loss of *TP53* and *RB1* (Fig. 4A). Furthermore, *SOX2* silencing restored sensitivity to enzalutamide in vitro and in a mouse xenograft model (Fig. 4, B and C). Additionally, overexpression of Flag-tagged SOX2 in parental LNCaP/AR cells was sufficient to upregulate many of the basal and neuroendocrine lineage markers at levels comparable to that seen with *TP53* and *RB1* knockdown and to confer enzalutamide resistance in vitro (fig. S11, A and B). Having identified *SOX2* as a driver of lineage plasticity, we considered the possibility that other iPS factors may play a similar role. *OCT4* and *KLF4*, but not *MYC*, were upregulated after knockdown of *TP53* and *RB1*, but neither gene alone or in combination conferred resistance to enzalutamide (fig. S11, C and D).

Taken together, these data establish a critical role for *TP53*, together with *RB1*, in maintaining prostate luminal cell identity and define a mechanism, through up-regulation of *SOX2*, whereby tumor cells acquire lineage plasticity as a means to escape luminal-specific drug therapy targeted against AR. Therefore, the ~50% frequency of *TP53* deletion or mutation in metastatic CRPC tumors (often with concurrent mutations in *RB1* and/or *PTEN*) is likely to have clinical implications for response to antiandrogen therapy and for subsequent mechanisms of relapse. Specifically, we propose that tumors with intact *TP53* and *RB1* are likely to acquire resistance by restoration of AR signaling, whereas those with deficient *TP53* and *RB1* are more likely to escape therapy by transitioning away from an AR-dependent luminal identity through the reprograming activity of *SOX2* (Fig. 4D). There is precedent for TP53 and RB1 playing similar roles in maintaining fibroblast lineage commitment, based on evidence that efficiency of generating iPS cells from fibroblasts is

enhanced by the loss of function of either gene (23–25). In mouse models, *Tp53* and *Rb1* are also critical for maintenance of lineage identity in various cancers, such as hepatocellular carcinoma (26) and osteosarcoma (27).

The term “transdifferentiation” is often used to refer to lineage transitions where tumors with neuroendocrine features emerge from epithelial cancers. The model of drug resistance proposed here does not require tumor cells to transdifferentiate to an entirely new lineage. Instead, we suggest that the loss of *TP53* and *RB1* establishes a state of lineage plasticity (a multi-lineage, progenitor-like transition state), whereby tumor cells acquire the flexibility to transition to alternative lineages when faced with selective pressure. In the setting of antiandrogen therapy, the critical requirement for drug resistance is a loss of luminal identity, which may eventually manifest through outgrowth of more classical basal, mesenchymal, or neuroendocrine-like cancers. A critical feature of this model is that antiandrogen therapy serves as selective pressure, rather than a driver of lineage plasticity as proposed by others (18). Whether the progenitor-like transition state induced by SOX2 in the setting of *TP53* and *RB1* loss reflects a normal cell type present during the development of the prostate gland or an aberrant cell type only observed in cancer remains to be defined.

The lineage plasticity described here, together with observations of intratumoral heterogeneity from genomic sequencing analysis (28), presents major therapeutic challenges. Our observation that antiandrogen resistance can be reversed by inhibiting SOX2 raises some hope that appropriate clinical interventions could prevent or overcome resistance. Direct pharmacologic inhibition of SOX2 is not feasible currently, but it may be possible to prevent *SOX2* transcriptional up-regulation following the loss of *TP53* and *RB1*. Although the details of *SOX2* upregulation in prostate cancer remain to be defined, there are clear mechanisms of RB1 and TP53 regulation of SOX2 in fibroblasts that could be relevant. RB1 directly represses SOX2 by recruitment to E2F binding sites in the *SOX2* promoter, where it creates repressive chromatin marks (24). TP53 indirectly inhibits SOX2 by up-regulation of its target gene *miR-34* that targets *SOX2* mRNA (29). Careful elucidation of the *SOX2* chromatin landscape across various stages of prostate cancer might yield specific strategies to block expression with inhibitors of appropriate chromatin-modifying enzymes.

Supplementary Material

Refer to Web version on PubMed Central for supplementary material.

Acknowledgments

We thank members of the Sawyers lab for helpful discussions, M. Nevalainen (Milwaukee, Wisconsin) for providing CWR22Pc cells, J. Zuber (Vienna, Austria) for providing retroviral- and lentiviral miR-E–based expression vectors, W. Wu for the artwork in Fig. 4D, S. Deng for taking confocal microscopy images of fig. S5C, N. Fan for assistance with tissue processing, and Immunohistochemistry and the Antitumor Assessment Core for technical assistance with xenograft experiments. P.M. was supported by the Congressionally Directed Medical Research Programs Prostate Cancer Research Program Postdoctoral Training Award PC141607. C.L.S. is funded by the Howard Hughes Medical Institute (SU2C/American Association for Cancer Research) (grant DT0712), the U.S. National Cancer Institute (NCI) of the NIH (grants R01 CA155169-04 and R01 CA19387-01), NIH/NCI/Memorial Sloan Kettering Cancer Center (MSKCC) Spore in Prostate Cancer (grant P50 CA092629-14), and the NCI/MSKCC Support Grant/Core Grant (P30 CA008748-49 and P3 CA008748-49 S2). M.A.R., H.B., and F.D. are funded by NIH grant R01CA116337 and the Prostate Cancer Foundation, and H.B. and M.A.R. received support from the Starr Cancer Consortium. F.D. is also funded by European Research Council ERCCoG648670. H.B. is

also funded by Damon Runyon Cancer Research Foundation grant CI-67-13 and U.S. Department of Defense grant PC121341. D.W.G. is funded by NCI grants CA179907 and CA009072. E.d.S. is funded by NCI grant P30 CA008748 and NIH grant U54OD020355. C.L.S. and J.W. are co-inventors of enzalutamide and may be entitled to royalties. Enzalutamide is commercially available from Selleck Chemicals. C.L.S. serves on the board of directors of Novartis and is a paid consultant to ORIC Pharmaceuticals.

REFERENCES AND NOTES

1. Pao W, et al. PLOS Med. 2005; 2:e73. [PubMed: 15737014]
2. Gorre ME, et al. Science. 2001; 293:876–880. [PubMed: 11423618]
3. Lito P, Rosen N, Solit DB. Nat. Med. 2013; 19:1401–1409. [PubMed: 24202393]
4. Sequist LV, et al. Sci. Transl. Med. 2011; 3:75ra26.
5. Beltran H, et al. Cancer Discov. 2011; 1:487–495. [PubMed: 22389870]
6. Robinson D, et al. Cell. 2015; 161:1215–1228. [PubMed: 26000489]
7. Watson PA, Arora VK, Sawyers CL. Nat. Rev. Cancer. 2015; 15:701–711. [PubMed: 26563462]
8. Meyers FJ, et al. Cancer. 1998; 83:2534–2539. [PubMed: 9874460]
9. Tran C, et al. Science. 2009; 324:787–790. [PubMed: 19359544]
10. Balbas MD, et al. eLife. 2013; 2:e00499. [PubMed: 23580326]
11. Arora VK, et al. Cell. 2013; 155:1309–1322. [PubMed: 24315100]
12. Beltran H, et al. Nat. Med. 2016; 22:298–305. [PubMed: 26855148]
13. The Cancer Genome Atlas Research Network. Cell. 2015; 163:1011–1025. [PubMed: 26544944]
14. Aparicio AM, et al. Clin. Cancer Res. 2016; 22:1520–1530. [PubMed: 26546618]
15. Tan H-L, et al. Clin. Cancer Res. 2014; 20:890–903. [PubMed: 24323898]
16. Zhou Z, et al. Cancer Res. 2006; 66:7889–7898. [PubMed: 16912162]
17. Gazdar AF, et al. J. Thorac. Oncol. 2015; 10:553–564. [PubMed: 25675280]
18. Kregel S, et al. PLOS ONE. 2013; 8:e53701. [PubMed: 23326489]
19. Takahashi K, Yamanaka S. Nat. Rev. Mol. Cell Biol. 2016; 17:183–193. [PubMed: 26883003]
20. Rudin CM, et al. Nat. Genet. 2012; 44:1111–1116. [PubMed: 22941189]
21. Bass AJ, et al. Nat. Genet. 2009; 41:1238–1242. [PubMed: 19801978]
22. Russo MV, et al. Oncotarget. 2016; 7:12372–12385. [PubMed: 26540632]
23. Hong H, et al. Nature. 2009; 460:1132–1135. [PubMed: 19668191]
24. Kareta MS, et al. Cell Stem Cell. 2015; 16:39–50. [PubMed: 25467916]
25. Li H, et al. Nature. 2009; 460:1136–1139. [PubMed: 19668188]
26. Tschaharganeh DF, et al. Cell. 2014; 158:579–592. [PubMed: 25083869]
27. Calo E, et al. Nature. 2010; 466:1110–1114. [PubMed: 20686481]
28. Gerlinger M, et al. N. Engl. J. Med. 2012; 366:883–892. [PubMed: 22397650]
29. Choi YJ, et al. Nat. Cell Biol. 2011; 13:1353–1360. [PubMed: 22020437]
30. Zhang D, et al. Nat. Commun. 2016; 7:10798. [PubMed: 26924072]

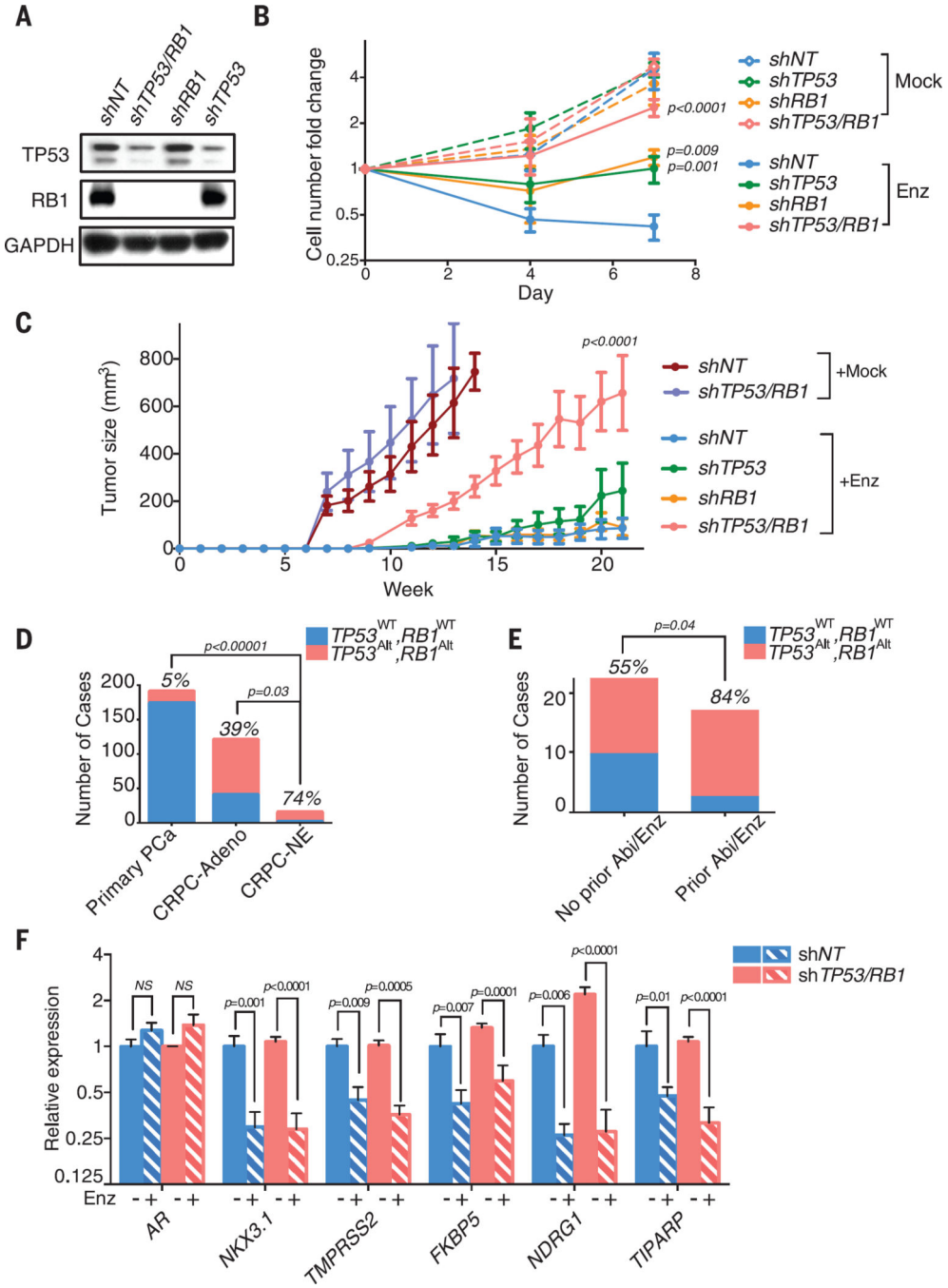

Fig. 1. Combined *TP53* and *RB1* loss of function confers enzalutamide resistance

(**A**) Western blot showing TP53 and RB1 protein levels in LNCaP/AR cells transduced with annotated hairpins. Glyceraldehyde-3-phosphate dehydrogenase (GAPDH) served as a loading control. (**B**) Growth curve of LNCaP/AR cells transduced with annotated hairpins in charcoal-stripped serum (CSS) medium, following LNCaP/AR protocol B (see materials and methods). Enz denotes 10-μg/ml enzalutamide treatment. Mock denotes the equivalent volume of dimethyl sulfoxide (DMSO) treatment. (**C**) Tumor growth curve of xenografted LNCaP/AR cells transduced with annotated hairpins. +Enz denotes enzalutamide treatment

at 10 mg/kg orally 1 day after grafting. +Mock denotes DMSO treatment at the same dosage. (**D**) Number of cases of co-occurrence of *TP53* and *RB1* alterations in primary prostate cancer (PCa), CRPC with adenocarcinoma histology (CRPC-Adeno), and CRPC with neuroendocrine-like histology (CRPC-NE) ($n = 559$). The genomic status of the two genes was assessed from whole-exome sequencing data, as in (12). *P* values were calculated using Fisher's exact test. The percentage of cases with alterations in both *TP53* and *RB1* in primary PCa, CRPC-Adeno, and CRPC-NE is shown. (**E**) Number of cases with $TP53^{Alt}$, $RB1^{Alt}$, based on whether the patient had already received therapy with enzalutamide or abiraterone (Abi/Enz) ($n = 44$ cases: 14 cases in the $TP53^{WT}$, $RB1^{WT}$ group and 30 cases in the $TP53^{Alt}$, $RB1^{Alt}$ group). *P* values were calculated using Fisher's exact test. (**F**) Relative gene expression of *AR* and *AR* target genes in tumors collected from the LNCaP/AR xenograft model. Enz denotes enzalutamide treatment at 10 mg/kg from day 1 of grafting. Minus signs denote DMSO treatment at the same dosage. For all panels unless otherwise noted, mean ± SEM (error bars) is represented, and *P* values were calculated using multiple *t* tests. NS, not significant.

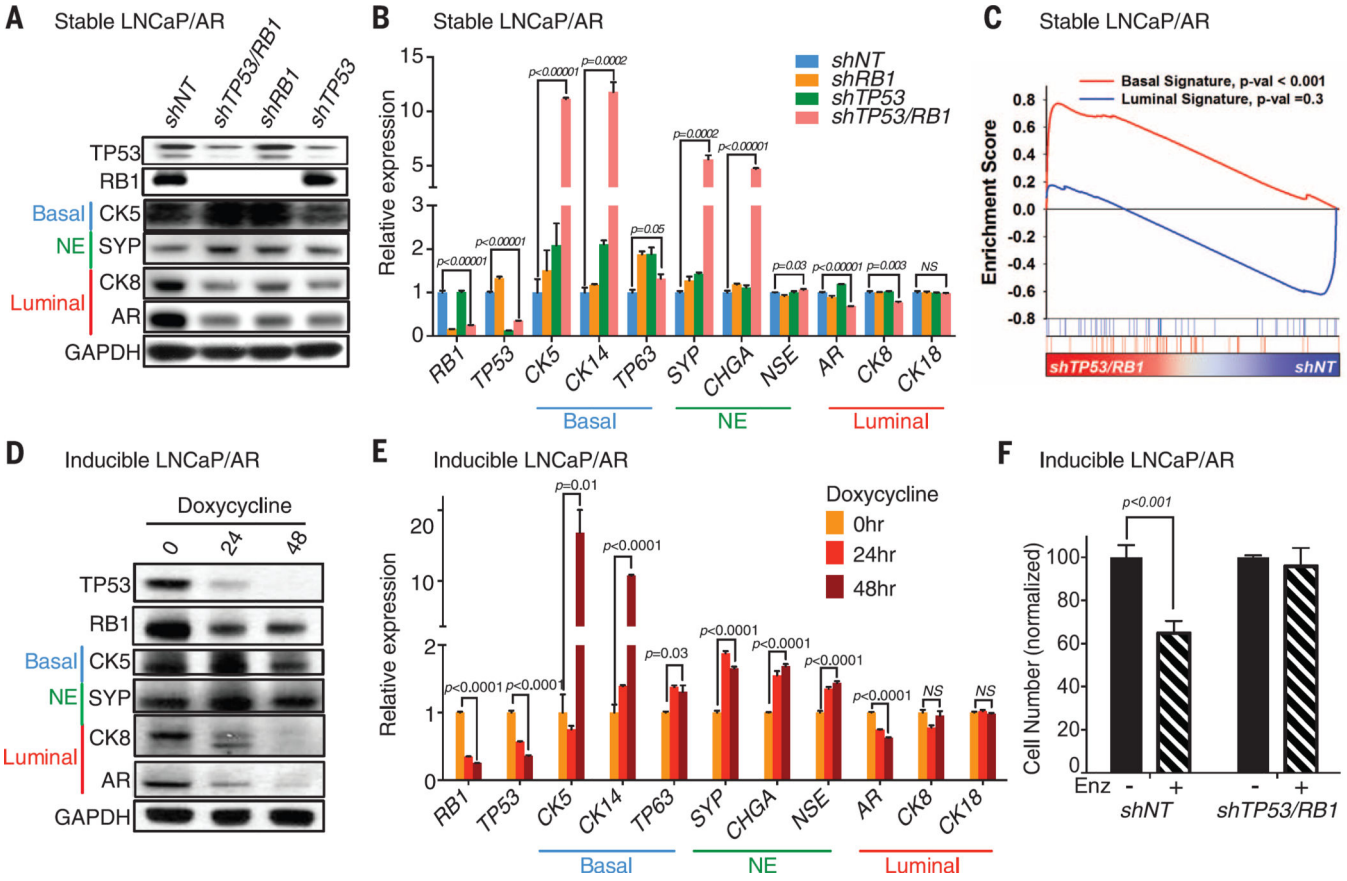

Fig. 2. Combined *TP53* and *RB1* loss of function leads to increased lineage plasticity

(**A**) Western blot of selected cellular lineage markers in LNCaP/AR cells transduced with annotated hairpins in a stable vector system. GAPDH served as a loading control. (**B**) Relative gene expression of lineage markers in LNCaP/AR cells transduced with annotated hairpins in a stable vector system. (**C**) Expression of luminal- and basal-signature genes [as defined in table S1 and (30)] was compared in LNCaP/AR cells transduced with annotated hairpins (sh*TP53/RB1* versus sh*NT*) by gene set enrichment analysis. (**D**) Western blot showing protein levels of selected lineage markers in LNCaP/AR cells transduced with hairpins against *TP53* and *RB1* in an inducible vector system at various time points. GAPDH served as a loading control. (**E**) Relative gene expression of lineage markers in LNCaP/AR cells transduced with hairpins against *TP53* and *RB1* in an inducible vector system at various time points. (**F**) Cell number of LNCaP/AR cells transduced with annotated hairpins in an inducible vector system, normalized to the −Enz group. Cells were treated with doxycycline for 48 hours and then treated with 7 days of enzalutamide in CSS medium, following LNCaP/AR protocol A. +Enz denotes 10-μg/ml enzalutamide treatment; −Enz denotes DMSO treatment with same volume as enzalutamide. For all panels unless otherwise noted, mean ± SEM (error bars) is represented, and *P* values were calculated using multiple *t* tests. NS, not significant. Cell types that express each set of lineage markers are indicated with different colors.

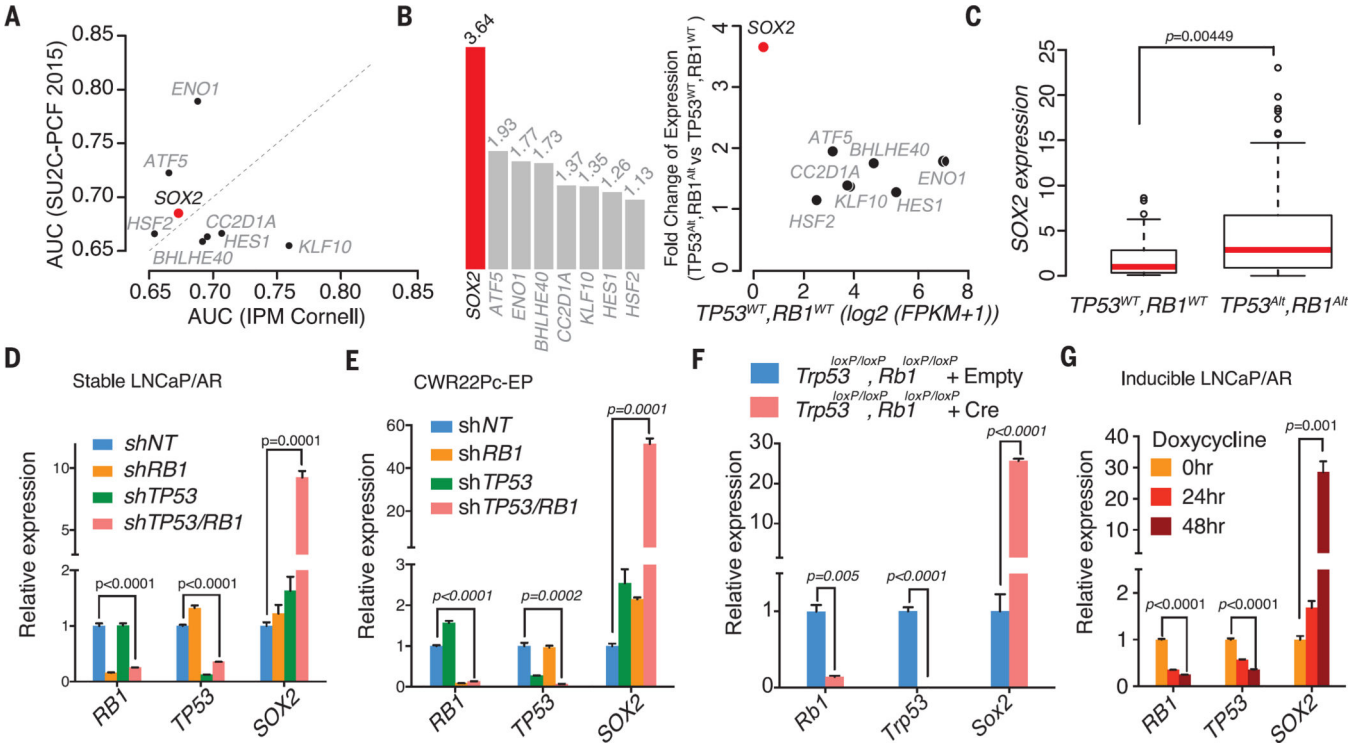

Fig. 3. Elevation of *SOX2* gene expression is highly correlated with the inactivation of *TP53* and *RB1*

(**A**) Area under the curve (AUC)–based analysis indicating transcription factors (TFs) overexpressed in the *TP53*- and *RB1*-altered phenotype in both the CRPC patients from IPM-Cornell (12) and the SU2C–Prostate Cancer Foundation (PCF) 2015 cohorts (6) (AUC ≥ 0.65). (**B**) (Left) Fold change (FC) of transcript levels of the identified TFs in *TP53*- and *RB1*-altered versus *TP53* and *RB1* WT samples. Median values are shown. (Right) FC of identified TFs versus normalized expression in *TP53* and *RB1* WT samples, expressed as $\log_2$(FPKM+1). FPKM, fragments per kilobase of transcript per million mapped reads. The *y* axis serves both the left and right panels. (**C**) Relative expression of *SOX2* in *TP53*- and *RB1*-altered and *TP53* and *RB1* WT samples for the IPM-Cornell (n = 35) (12) and SU2C-PCF 2015 (n = 77) data sets (6). For each cohort, data are scaled to the median of the *TP53* and *RB1* WT status. *P* value is Wilcoxon-Mann-Whitney, with lower and upper whiskers corresponding to the minimum and maximum nonoutlier values of the data distribution, respectively. (**D**) Relative gene expression of *TP53, RB1*, and *SOX2* in LNCaP/AR cells transduced with annotated hairpins in a stable vector system. (**E**) Relative gene expression of *TP53, RB1*, and *SOX2* in CWR22Pc-EP cells transduced with annotated hairpins in a stable vector system. (**F**) Relative gene expression of *Trp53, Rb1*, and *Sox2* in $Trp53^{loxP/loxP}$, $Rb1^{loxP/loxP}$ mouse organoids transduced with annotated Cre or empty vector. (**G**) Relative gene expression of *TP53, RB1*, and *SOX2* in LNCaP/AR cells transduced with annotated hairpins in an inducible vector system at various time points. For all panels unless otherwise noted, mean ± SEM (error bars) is represented, and *P* values were calculated using multiple *t* tests.

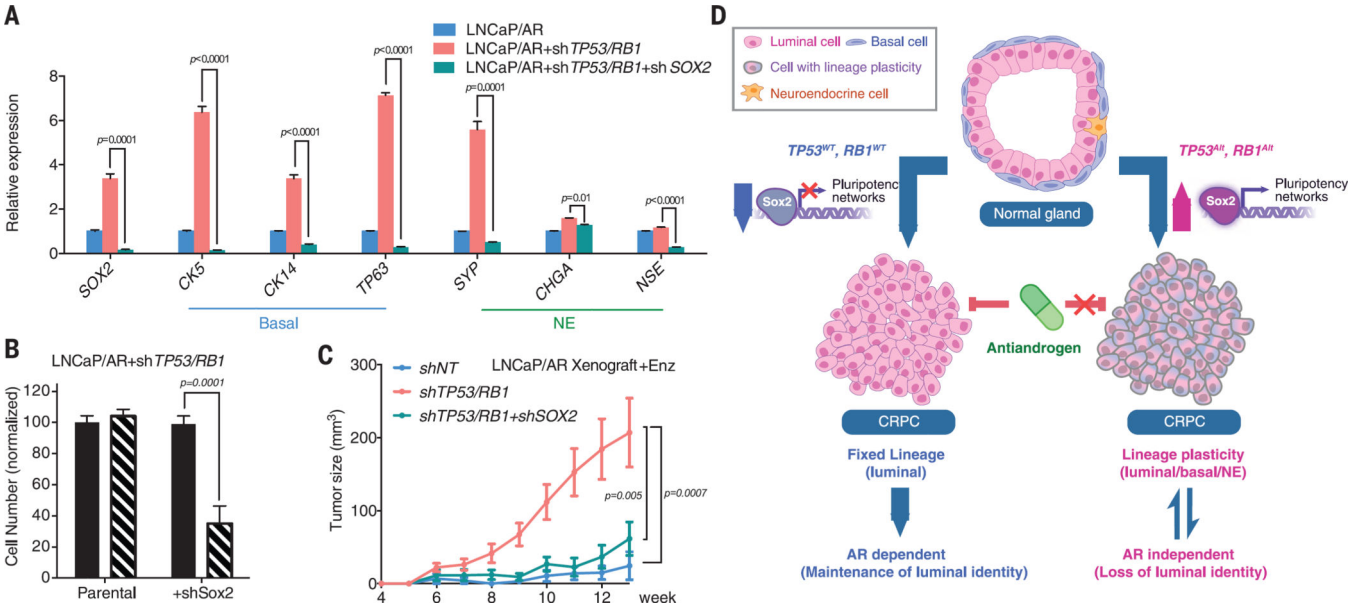

Fig. 4. *SOX2* is required for lineage plasticity and enzalutamide resistance induced by inactivation of *TP53* and *RB1*

(**A**) Relative gene expression of *SOX2* and lineage marker genes in LNCaP/AR cells transduced with annotated hairpins in a stable vector system. (**B**) Cell numbers of LNCaP/AR transduced with annotated hairpins (sh*TP53* and *RB1* versus sh*TP53* and *RB1*+sh*SOX2*), normalized to the parental −Enz group. Cells were treated for 7 days with enzalutamide or DMSO in CSS medium, following LNCaP/AR protocol A. (**C**) Tumor growth curve of xenografted LNCaP/AR cells transduced with annotated hairpins. +Enz denotes enzalutamide treatment at 10 mg/kg orally 1 day after grafting. For panels (A) to (C) unless otherwise noted, mean ± SEM (error bars) is represented and *P* values were calculated using multiple *t* tests. (**D**) Model depicting the lineage plasticity change and antiandrogen resistance in CRPC-Adeno due to *TP53* and *RB1* alterations ($TP53^{Alt}$, $RB1^{Alt}$) compared to CRPC-Adeno with WT *TP53* and *RB1* ($TP53^{WT}$, $RB1^{WT}$).